Nonresonant inelastic x-ray scattering study of cubic boron nitride

S. Galambosi, J. A. Soininen, and K. Hämäläinen
Department of Physics, POB 64, University of Helsinki, FIN-00014 Helsinki, Finland

Eric L. Shirley
Optical Technology Division, Physics Laboratory, National Institute of Standards and Technology, Gaithersburg, Maryland 20899

C.-C. Kao
National Synchrotron Light Source, Brookhaven National Laboratory, Upton, New York 11973
(Received 22 January 2001; published 18 June 2001)

The dynamic structure factor of cubic boron nitride has been measured using nonresonant inelastic x-ray scattering. The experimental data are compared with the results of a recently developed *ab initio* calculation scheme, which takes into account the interaction between the excited electron and the hole. The agreement between the experiment and theory is good over an extended momentum transfer range, which emphasizes the importance of proper inclusion of the electron-hole interaction. The results are also compared with a reflectance measurement that represents the zero-momentum-transfer limit. The complementary nature of these different experimental methods is discussed in view of the *ab initio* calculations.

DOI: 10.1103/PhysRevB.64.024102 PACS number(s): 78.70.Ck, 71.15.−m, 71.20.−b

I. INTRODUCTION

We have conducted a combined experimental and theoretical study of the dynamic structure factor of single crystal cubic boron nitride (cBN) using nonresonant inelastic x-ray scattering (NRIXS). Recently boron nitride has been extensively studied by numerous experimental techniques because it exhibits several fascinating characteristics such as semiconducting properties with a large band gap. The interest is partially due to the fact that cubic boron nitride and diamond have many very similar properties. They have similar lattice constants, being in the diamond and zinc blende crystal structures, respectively. Both materials have low densities, and high thermal conductivities, electrical resistivities, and melting points. This has caused both materials to be considered as candidates for high-temperature electronics, although the potential for *n*- and *p*-type doping is much more promising in cBN. Conversely, it can be difficult to grow cBN crystals in the zinc blende structure. Because of the lattice constants being similar, cBN is considered also as a candidate material for growing diamond thin films.

The optical properties of cBN have also drawn both experimental[1–3] and theoretical[4] interest. The computational part of this work is based on an *ab initio* scheme[5,6] that takes into account the interaction of the excited electron and the hole. The scheme was originally developed for studying the optical properties of solids and later extended to NRIXS.[7,8] This scheme, as well as others based on the same formalism,[9] has proven reliable in the study of the optical properties for a wide range of materials. It has also been used to model absorption in cBN,[10] where comparison with experimental reflectance data[2] has revealed some discrepancies. This has motivated us to study this system with NRIXS, which can access the dynamic structure factor with a finite momentum transfer. The experimental method has been shown to give reliable results for a wide variety of materials.[11] A very recent study on lithium fluoride and diamond[7] shows the versatility of this technique accessing, for example, an indirect band gap. The goals of this study are (i) to study the momentum-transfer dependence of the dielectric response of cBN and (ii) to complement and verify the findings of the experimental absorption studies and the theoretical results.

In what follows, we first give some basic relationships of NRIXS related to our computational scheme. After discussing experimental details, we report the main experimental results. Finally, we compare NRIXS calculations and experimental results with their optical counterparts.

II. INELASTIC X-RAY SCATTERING

The double differential cross section of inelastic x-ray scattering is directly proportional to the dynamic structure factor $S(\mathbf{q},\omega)$

$$\frac{d^2\sigma}{d\Omega d\omega} = (d\sigma/d\Omega)_{\mathrm{Th}} S(\mathbf{q},\omega), \tag{1}$$

where $\mathbf{q}$ and ω are the momentum and energy transfers from the photon to the electrons of the system, respectively. The photon-electron interaction is described by the Thomson cross section $(d\sigma/d\Omega)_{\mathrm{Th}} = r_0^2(\bar{\epsilon}_1 \cdot \bar{\epsilon}_2)^2 \omega_2/\omega_1$, where r_0 is the classical electron radius, and ω_1 (ω_2) and $\bar{\epsilon}_1$ ($\bar{\epsilon}_2$) are the energy and the polarization vector of the incident (scattered) photon. By measuring the energy transfer and changing the transferred momentum via the scattering angle, one can selectively study the various excitations produced in the sample. For solids, the low-momentum transfer ($<$ a few Å^{-1}) and low-energy transfer (<50 eV) region of $S(\mathbf{q},\omega)$ is dominated by valence electron excitations. In this region the dynamic structure factor can be written in terms of the macroscopic dielectric function ε_M

$$S(\mathbf{q},\omega)=\frac{q^2}{4\pi^2 n}\mathrm{Im}\left[\frac{-1}{\varepsilon_M(\mathbf{q},\omega)}\right], \tag{2}$$

where n is the average electron density in the solid. The dielectric function ε_M describes the response of the system to the total macroscopic electric field. The dynamic structure factor can be directly probed with NRIXS and ε_M can be calculated with the aid of the Kramers-Kronig transformations.

III. COMPUTATIONAL SCHEME

In principle, calculation of the macroscopic dielectric function ε_M would require the solution of the equations of motion (EOM) for the electron-hole pair operator, a typical equation being

$$\langle\Phi|[\hat{H},\hat{a}_c^\dagger\hat{a}_v]|0\rangle=E\langle\Phi|\hat{a}_c^\dagger\hat{a}_v|0\rangle. \tag{3}$$

Here $\hat{H}$ is the exact Hamiltonian of the many-body system, $\hat{a}_c^\dagger\hat{a}_v$ is an electron-hole pair creation operator, and $|\Phi\rangle$ is an exact excited state with energy E. Using the Tamm-Dancoff approximation (TDA),[12] we can extract an effective Hamiltonian H_{eff} from the EOM. In the Tamm-Dancoff approximation the excited state is assumed to be a combination of singly excited states, and in the ground state $|0\rangle$ only the valence states are occupied. The effective Hamiltonian contains single-particle terms (for both the electron and the hole) and electron-hole interaction terms. The interaction includes both the attractive ''direct'' interaction and the repulsive ''exchange'' interaction. This method has previously been used to analyze absorption and inelastic x-ray scattering experiments.[5–8]

Within linear-response theory, the macroscopic dielectric function of the system can be written as

$$\varepsilon_M(\mathbf{q},\omega)=1-\frac{4\pi}{q^2}\left\langle 0\left|\hat{\rho}_{\mathbf{q}}\frac{1}{\omega-\hat{H}_{\mathrm{eff}}+i\eta}\hat{\rho}_{\mathbf{q}}^\dagger\right|0\right\rangle, \tag{4}$$

where $\rho_{\mathbf{q}}^\dagger$ is the density-fluctuation operator. The resolvent $(\omega-\hat{H}_{\mathrm{eff}}+i\eta)^{-1}$ in Eq. (4) is calculated using an iterative Lanczos method. A detailed review of this scheme can be found in Refs. 5,6 and on its application to NRIXS in Refs. 7,8. As an input for studying cBN this scheme requires the *GW* band structure,[4] the single-particle wave functions taken from LDA pseudopotential[13,14] calculations, and the infrared dielectric constant ϵ_∞ (taken to be 4.46).

When comparing calculation results quantitatively to measurement, it is relevant to assess the expected accuracy of the theoretical spectra. Systematic shortcomings of the approximations used can at best be estimated by comparison to measurement, whereas numerical convergence of the present results is substantially better than the level of disagreement from experiment.

IV. EXPERIMENTAL DETAILS

The experiments were performed on beamline X21A at the National Synchrotron Light Source at the Brookhaven National Laboratory. The x rays were produced by a 27-pole hybrid wiggler and monochromatized using a four-bounce monochromator based on two separate and asymmetrically cut channel-cut Si crystals using (220) reflections. The incident energy resolution was approximately 0.2 eV at 8 keV. The monochromatic x rays were focused onto the sample using a double-focusing toroidal mirror with a platinum coating. The spot size was approximately 0.5 mm (horizontal) $\times 0.2$ mm (vertical). A detailed description of the experimental setup can be found in Refs. 15,16.

The scattered photons were analyzed using a spherically bent Si(444) crystal within the Rowland-circle geometry with a bending radius of 1 m. The active area of the analyzer crystal was limited to 36 mm of diameter in order to improve the energy resolution and simultaneously limit the spread of the scattering angles. The energy transfer scan was performed utilizing the so-called inverse-energy scan technique, i.e., keeping the scattered energy fixed (corresponding to a fixed analyzer angle of 86° close to back scattering in order to improve the energy resolution) while scanning the incident energy. Finally, the photons were detected by a very low-noise Si pin-diode detector. The total energy resolution of 0.4 eV at 7.92 keV was determined from the full width at half maximum (FWHM) of the quasielastic line.

The momentum transfer is determined by the scattering angle 2θ as $q\approx 4\pi/\lambda\sin\theta$, where $\lambda=2\pi c/\omega_1$ is the wavelength of the incident radiation, which varies by less than 5% in the energy range of interest. The momentum resolution is dominated by the finite size of the analyzer crystal and the relative uncertainty of the momentum transfer $\Delta q/q$ varied between 1.0 at $q=0.28$ Å^{-1} $(0.16\Gamma X)$ and 0.11 at $q=2.46$ Å^{-1} $(1.42\Gamma X)$.

The boron nitride sample was prepared using the temperature-difference method at high pressure (5 GPa) and at 2000 K.[1] The size of the sample was 2 mm$\times$2 mm $\times$0.4 mm and it was positioned in a vacuum chamber throughout the experiment. Another vacuum chamber was used between the sample, analyzer and detector to minimize air absorption and scattering. The measurements were performed by varying the momentum transfer along three main crystallographic directions [along the Cartesian directions (1,0,0), (1,1,0), and (1,1,1), corresponding to $\mathbf{q}\|\Gamma X$, ΓK, and ΓL, respectively] of the conventional cubic unit cell, with several different momentum transfer values for each direction. All desired directions of the momentum transfer were accessed by rotating the same single crystal with respect to the incident beam and scattering plane. The proper orientation was always found by observing appropriate Bragg reflections.

Several scans were performed for each $\mathbf{q}$, and the quasielastic line was measured between each scan in order to check the stability of the incident energy. The total shift was observed to be less than 0.1 eV between individual scans. Since the sample was thin enough, the low absorption enabled us to collect the data in the transmission geometry using a $(\theta,2\theta)$ scan. Within this arrangement the *direction* of momentum transfer was kept fixed along the chosen crystallographic axis while the *absolute value* $q=|\mathbf{q}|$ was varied by changing the scattering angle. The experimental data were

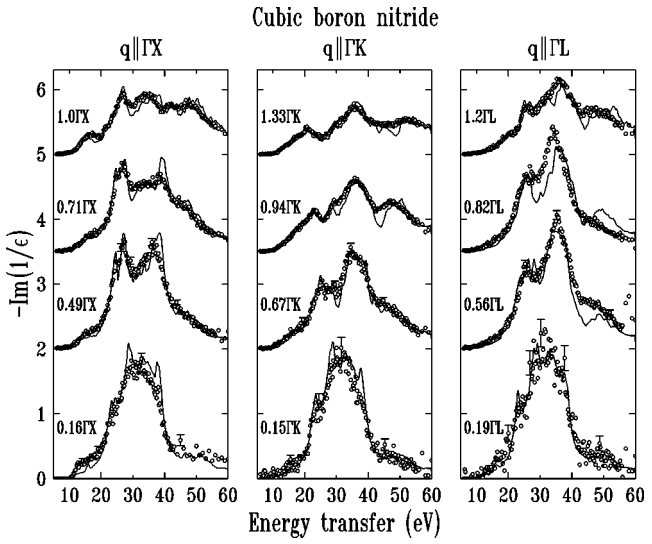

FIG. 1. The experimental (circles) and the theoretical (solid line) dynamic structure factor for cubic boron nitride along three different crystallographic directions. The magnitudes of momentum transfers are given in the figure relative to the corresponding symmetry points. Selected error bars ($\pm\sigma$) are shown for the two lowest momentum transfer spectra, whereas the error bars in the higher momentum transfer spectra are equal to or smaller than the size of the symbol.

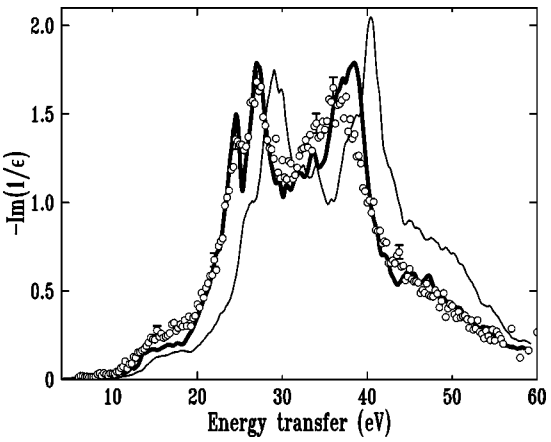

FIG. 2. The experimental (circles) and the theoretical dynamic structure factor for cubic boron nitride with momentum transfer $\mathbf{q}=0.49\Gamma X$. Typical $\pm\sigma$ error bars are shown. Results of calculations with (thick solid line) and without (thin solid line) the electron-hole interaction are shown.

corrected for the variation in the incident intensity (using an ion chamber as a beam monitor), monitor efficiency, sample self-absorption, air absorption, and the energy and polarization factors in the Thomson cross section. However, all of these factors contribute only a few percent over the observed energy transfer range. After the abovementioned corrections are applied, the experimental data can be very easily normalized to an absolute scale using the so-called *f*-sum rule[17]

$$\int_0^\infty d\omega\,\omega S(\mathbf{q},\omega)=\frac{q^2}{2}. \tag{5}$$

The upper limit of the integration was the same as the maximum energy transfer measured (typically 100 eV) except for the lowest momentum transfers, where the spectral weight of the dynamic structure factor is primarily concentrated at very low energy transfers.

V. RESULTS AND DISCUSSION

The experimental data along three main crystallographic axes together with our *ab initio* calculations for various momentum transfer values are shown in Fig. 1. The theoretical curves are convolved with our experimental energy resolution of 0.4 eV. Clear directional differences are observed, and the differences are more pronounced at higher momentum transfer. The general agreement between experiment and theory over extended momentum-transfer range is remarkable. It should be noted that both curves are on an absolute scale and that no energy-scale shifts are introduced. Generally such shifts would be necessary in order to improve the agreement with the theory if the latter lacked a proper treatment of electron-hole interaction. The effects of the electron-hole interaction is illustrated in Fig. 2, which shows the comparison between theoretical loss functions computed with and without the electron-hole interaction and the experimental loss function. The effect of the electron-hole interaction is not merely a simple shift of the energy scale (which in the case of cBN would be about 3 eV). The effect could also be seen empirically as a relative intensity change for various peaks and a splitting and merging of various double-peaked structures. However, there is really no one-to-one correspondence between spectral features in ''interacting'' and ''noninteracting'' spectra.

It can be seen in Fig. 1 that at low momentum transfers the dynamic structure factor consists of a relatively narrow feature approximately 20 eV wide. As the momentum transfer is increased, the spectra broaden and the peaks smooth out. This can be understood as a signature of the fact that both energy and momentum are conserved in the scattering process. For the lowest momentum transfers there are several peaks present in the theoretical spectra. Three of them (located at 28.5, 33.0, and 38.0 eV) were labeled as plasmons in earlier calculations on cBN (Ref. 18) (their corresponding energies were 27.3, 32.5, and 38.5 eV). These peaks are not visible in the experimental results, perhaps because of the statistical error. At higher momentum transfers there are several clearly defined structures visible in the experimental spectra. The dispersion of these features can be seen in Fig. 1. From the theoretical calculations of ε_M we deduce that these features usually originate from the combined structure of $\mathrm{Re}(\varepsilon_M)$ and $\mathrm{Im}(\varepsilon_M)$, so a simple critical-point or band-structure analysis of the features is not feasible. There are, however, some structures that can be considered as well defined elementary excitations. For example, the double peak structure (peaks at 25 and 27 eV) in the theoretical data for the momentum transfer $0.49\Gamma X$ can be considered as plasmons [i.e., zero crossings of $\mathrm{Re}(\varepsilon_M)$]. This structure may also be present in the experimental spectrum, although the

low-energy peak appears to be a broad shoulder. When compared to the experimental values, the theoretical calculation reproduces the energies of these peak structures within 0.5 eV, although some discrepancy remains, mostly in the intensities and widths.

Since the electronic structure, dielectric and optical properties of cBN and diamond are very similar, it is interesting to compare them in light of their band structure and inelastic scattering spectra. A key difference of relevance is the nature of the low-lying conduction bands along the ΓX direction. Because cBN has the zinc blende structure, it lacks the full symmetry of diamond, so that the lowest two conduction bands at X are not degenerate in cBN, whereas they are in diamond. Concomitantly, the conduction-band minimum in cBN is at X, rather than near X along the ΓX line. Furthermore, because of the difference in symmetry, there is no Brillouin-zone selection rule that governs observation of the indirect band gap in cBN, whereas the band gap in diamond is not seen in the first Brillouin zone, but only in the second, because of diamond's symmetry. However, the inelastic scattering features involving the indirect band gap are very weak features in the spectra. To a large degree, the inelastic scattering spectra of cBN show similar trends as diamond for scattering along the ΓX and ΓL lines.[19] Effects of the different conduction band minima are also noticeable in the case of resonant x-ray scattering, because of the high degree of band parallelism between the valence and the conduction bands near X in cBN that is absent in diamond. As a consequence, it appears that final-state valence hole effects can strongly affect the emission spectra in cBN.[20]

The experimental data and theoretical calculations clearly show that at low momentum transfer the data lose directional dependence. At low q the imaginary part of the longitudinal dielectric function (measured in IXS) reduces (for cubic systems) to the imaginary part of the transverse dielectric function (measured in optical studies).[21] The only difference is that in the IXS case the reference direction of the sample is related to the direction of **q**, while in the absorption case it is related to the polarization direction of the incident beam. Therefore NRIXS can be utilized to study the optical properties of low-Z elements with hard x rays and bulk penetration.[22] This equivalence of NRIXS and absorption can be expanded even up to the x-ray absorption region.[23]

Cubic boron nitride has no large anisotropy in absorption compared to, for example, previously studied systems with hexagonal structure, where signatures because of π and σ bonding represent an extreme case.[17] Also, there is practically no change in the dynamic structure factor below the smallest momenta studied, which approximately correspond to the zero-momentum-transfer (optical) case, and whose results can directly be compared to optical measurements. Using much lower momentum values with NRIXS becomes experimentally infeasible, since the total cross section scales with q^2, and statistics become poor (which can already be seen as larger error bars for the lowest momentum transfer measurements in our case).

As shown previously, the dynamic structure factor is related to the inverse of the imaginary part of the dielectric function. However, present theoretical calculation produces the complex dielectric function and can be used to calculate also the reflectance. Therefore, NRIXS can be used indirectly to complement and verify reflectance experiments. Here, we have carried out a calculation for a momentum transfer of 0.10 Å^{-1} and converted the result into reflectance. This is compared with a reflectance measurement[2] and is shown in Fig. 3. The orientation of the sample is not reported in the article, so our theoretical curve displayed here is the average over three main crystallographic directions [along the Cartesian directions (1,0,0), (1,1,0), and (1,1,1)], but the effect of anisotropy here is only a few percent. There is a reasonably good general agreement between the theory and experiment over a large energy transfer range. A slight difference of the peak positions is visible. The main clear discrepancy appears at an energy transfer of roughly 7 eV. There, the experimental data show a prominent shoulder that is not reproduced in the theory, which we conjecture arises from phonon-assisted indirect transitions.

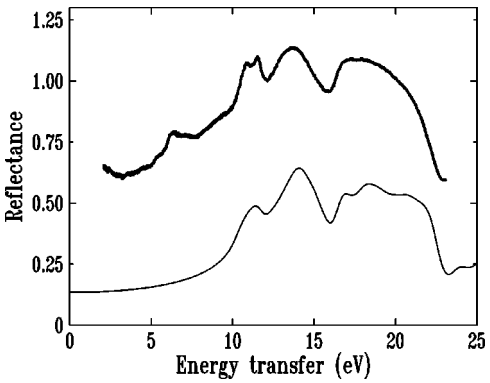

FIG. 3. The experimental reflectance from Ref. 2 (thick solid line) shown along with the present theoretical calculation based on the evaluation of the complete dielectric function at a small momentum transfer value (thin solid line). The experimental data is scaled to agree with the calculated reflectance.

VI. CONCLUSION

We have measured the dynamic structure factor of cubic boron nitride using nonresonant inelastic x-ray scattering. The experimental data are in a good accord with an *ab initio* theoretical calculation, which properly takes into account the electron-hole interaction. We have further applied the theoretical model to calculate the reflectance and compared to a previous measurement. The experimental reflectance is reproduced fairly well by our calculation, except for a feature at 7 eV energy transfer that we attribute to indirect transitions.

Nonresonant inelastic x-ray scattering is shown to be a competitive and complementary technique to probe dielectric response of insulators and semiconductors. The possibility to control both the energy and the momentum transfer over a wide range suggests a new way to look at the complete picture of electron dynamics in materials. Furthermore, the theoretical framework is shown to be well-suited to explain the observed rich details in the dynamic structure factor.

ACKNOWLEDGMENTS

The authors would like to acknowledge S. Shin for providing us the sample and W.A. Caliebe for useful discussions. This project was supported by the Academy of Finland (7379,39182,40732) and the U.S. Department of Energy (Grant No. W-31-109-ENG-38).

[1] A. Agui, S. Shin, M. Fujisawa, Y. Tezuka, T. Ishii, Y. Muramatsu, O. Mishima, and K. Era, Phys. Rev. B **55**, 2073 (1997).
[2] N. Miyata, K. Moriki, O. Mishima, M. Fujisawa, and T. Hattori, Phys. Rev. B **40**, 12 028 (1989).
[3] A. Onodera, M. Nakatani, M. Kobayashi, Y. Nisida, and O. Mishima, Phys. Rev. B **48**, 2777 (1993).
[4] M. P. Surh, S. G. Louie, and M. L. Cohen, Phys. Rev. B **43**, 9126 (1991).
[5] L. X. Benedict and E. L. Shirley, Phys. Rev. B **59**, 5441 (1999).
[6] L. X. Benedict, E. L. Shirley, and R. B. Bohn, Phys. Rev. B **57**, R9385 (1998); L. X. Benedict, E. L. Shirley, and R. B. Bohn, Phys. Rev. Lett. **80**, 4514 (1998).
[7] W. A. Caliebe, J. A. Soininen, E. L. Shirley, C.-C. Kao, and K. Hämäläinen, Phys. Rev. Lett. **84**, 3907 (2000).
[8] J. A. Soininen and E. L. Shirley, Phys. Rev. B **61**, 16 423 (2000).
[9] For a recent review see M. Rohlfing and S. G. Louie, Phys. Rev. B **62**, 4927 (2000); also see S. Albrecht, L. Reining, G. Onida, and R. del Sole, Phys. Rev. Lett. **80**, 4510 (1998); J. W. van der Horst, P. A. Bobbert, M. A. J. Michels, G. Brocks, and P. J. Kelly, *ibid.* **83**, 4413 (1999).
[10] E. L. Shirley (unpublished).
[11] B. C. Larson, J. Z. Tischler, E. D. Isaacs, P. Zschack, A. Fleszar, and A. G. Eguiluz, Phys. Rev. Lett. **77**, 1346 (1996); W. Schülke, K. Höppner, and A. Kaprolat, Phys. Rev. B **54**, 17 464 (1996); J. P. Hill, C.-C. Kao, W. A. Caliebe, D. Gibbs, and J. B. Hastings, Phys. Rev. Lett. **77**, 3665 (1996).
[12] See, for example, A. Fetter and J. D. Walecka, *Quantum Theory of Many Particle Systems* (McGraw-Hill, San Francisco, 1971), pp. 538–539.
[13] P. Hohenberg and W. Kohn, Phys. Rev. **136**, 864 (1964); W. Kohn and L. J. Sham, *ibid.* **140**, 1133 (1965).
[14] For a review, see W. E. Pickett, Comput. Phys. Rep. **9**, 115 (1989).
[15] W. A. Caliebe, C.-C. Kao, M. Krisch, T. Oversluizen, P. Montanez, and J. B. Hastings, *Synchrotron Radiation Instrumentation: Tenth U.S. National Conference*, edited by E. Fontes, AIP Conf. Proc. No. 417 (AIP, Woodbury, NY, 1997), p. 6.
[16] K. Hämäläinen, M. Krisch, W. Caliebe, and J. B. Hastings, Rev. Sci. Instrum. **66**, 1525 (1995); C.-C. Kao, K. Hämäläinen, M. Krisch, D. P. Siddons, T. Oversluizen, and J. B. Hastings, *ibid.* **66**, 1699 (1995).
[17] W. Schülke, U. Bonse, H. Nagasawa, A. Kaprolat, and A. Berthold, Phys. Rev. B **38**, 2112 (1988).
[18] Y.-N. Xu and W. Y. Ching, Phys. Rev. B **44**, 7787 (1991).
[19] W. A. Caliebe, Ph.D. thesis, University of Kiel, 1997.
[20] E. L. Shirley, J. A. Soininen, G. P. Zhang, J. A. Carlisle, T. A. Callcott, D. L. Ederer, L. J. Terminello, and R. C. C. Perera, J. Electron Spectrosc. Relat. Phenom. **114-116**, 939 (2001).
[21] D. Pines, *Elementary Excitations in Solids* (W. A. Benjamin, New York, 1963).
[22] Y. Mizuno and Y. Ohmura, J. Phys. Soc. Jpn. **22**, 445 (1967).
[23] K. Tohji and Y. Udagawa, Phys. Rev. B **39**, 7590 (1989).